Computational and Theoretical Chemistry 1063 (2015) 29–34

Contents lists available at ScienceDirect

Computational and Theoretical Chemistry

journal homepage: www.elsevier.com/locate/comptc

Structures, stabilities and properties of hollow $(Al_2O_3)_n$ clusters (n = 10, 12, 16, 18, 24 and 33): Studied with density functional theory

YongBing Gu [a], NaiXiao Xu [b], MengHai Lin [b], Kai Tan [b,*]

[a] Department of Chemistry, Lishui College, Lishui 323000, China
[b] Fujian Provincial Key Laboratory of Theoretical and Computational Chemistry, College of Chemistry and Chemical Engineering, Xiamen University, Xiamen 361005, China

ARTICLE INFO

Article history:
Received 11 October 2014
Received in revised form 21 March 2015
Accepted 22 March 2015
Available online 18 April 2015

Keywords:
Density functional calculations
Al_2O_3
Hollow nanoparticles

ABSTRACT

Following recent experimental work revealing the structural formation of hollow Al_2O_3 nanoparticles, we explored the most stable structures of several large clusters, $(Al_2O_3)_n$ (n = 10, 12, 16, 18, 24 and 33). Using density functional theory, a comparative study of three hollow models was performed: fullerene-like, bubble-like and polyhedral structures. Within the size range studied, the polyhedral structures were found to be more stable than the fullerene-like and bubble-like structures. The binding energy increase as the cluster size increases, implying the polyhedral hollow clusters become more stable during the hollow Al_2O_3 growth process. The highest intensity IR frequency of calculated IR spectra for polyhedral hollow $(Al_2O_3)_n$ agree well with the available bulk Al_2O_3 experimental results. Thus, this study may serve as good models for predicting or interpreting the properties of hollow Al_2O_3 nanoparticles.

1. Introduction

Hollow nanoparticles with well-defined structures and shapes have attracted much attention for application, for example, in catalysis, solar cells, optical devices and photonic crystal [1,2]. Various approaches have been developed for the preparation of hollow spheres of alumina in the past few years, including templates and hydrothermal methods [3,4]. In particular, Li et al. used Au@Al_2O_3 core–shell-isolated nanoparticles in shell-isolated nanoparticle-enhanced Raman spectroscopy (SHINERS) to detect binding events [5]. Although well controlled nanostructures have been developed for various applications, the atomic structure of Al_2O_3 nanoshell is still unclear. Thus, studies are required to understand the properties of hollow or spherical aluminum oxides nanomaterials.

From a theoretical viewpoint, most calculations performed for Al_2O_3 structures have been limited to relatively small size [6,7]. Woodley calculated the structures of $(Al_2O_3)_n$ with n = 1–5 using density functional theory (DFT), where the initial structures are located with an evolutionary algorithm [8]. Rahane et al. [9] derived the structures of $(Al_2O_3)_n$ with n = 1–10 using simulated annealing in conjunction with DFT. Li and Cheng [10] obtained the structures of $(Al_2O_3)_n$ (n = 1–7) clusters via a genetic algorithm. Moreover, fullerene-like Al_2O_3 clusters (which resemble bubble cluster, Euler cluster, spheroid or hollow cluster) have been predicted by Karasev et al. [11] Sun et al. studied on the $(Al_2O_3)_n$ ($n \leqslant 30$) cage and cage-dimer clusters, and found that $Al_{60}O_{90}$ fullerene acts as a stable shell [12]. We found that the core–shell structure of $(Al_2O_3)_n$ cluster was more favorable than cage and cage-dimer structures for intermediate sizes. However, we cannot exclude the possibility that there exist other types of cage structures in Al_2O_3 nanosystem, such as zeolite frames consisting of corner-sharing Alumina tetrahedra which form a three-dimensional network. Hamad and Catlow [13,14] reported their progress in modeling hollow clusters of a range of key inorganic materials. A perfect bubble structure was defined as a non-pentagonal-faced polyhedral structure, related to the numbers of tetragonal, hexagonal, and octagonal faces. Thus, for the clusters of greater than 1 nm in diameter, there are various kinds of cage structure possible for the hollow shell model.

In the present paper, the geometry, electronic structures and stability of $(Al_2O_3)_n$ (n = 10–33) cage clusters with different topological types are investigated by DFT calculations. It is determined that hollow clusters with appropriate cage motifs are most promising building unit for obtaining stable structures.

2. Computational details

Calculations were performed with the B3LYP hybrid exchange correlation functional, as implemented in the *Gaussian 09* package. The 6-31G(d) basis set was employed. For comparison, calculations were also performed using the DMol^3 code [15,16] with the

* Corresponding author.

http://dx.doi.org/10.1016/j.comptc.2015.03.027
2210-271X/

gradient-corrected PBE pure density functional [17,18] in combination with the all-electron double numerical (DND) basis sets. Geometry optimizations were performed with no constraints of freedom. The reported stationary points were confirmed to be local minima by harmonic vibrational analyses at the same theoretical level. The structure of a fully coordinated Al_2O_3 cluster may be represented by vertices (Al nuclei) connected with lines (oxygen bridges). Because of the different 2D ring-structured building units, there are three possible types of model structures (Scheme 1). In fullerene-like case, it follows from the Euler formula $n + f - e = 2$ (n: number of vertices; e:edges; f:faces) that there are exactly 12 pentagons in a fullerene and $n/2 - 10$ hexagons. For the bubble model, we also use Euler formula as discussed by Spano et al. [19]:

$$N_{6\_ring} = n - 4 - 2N_{8\_ring} \quad (1)$$

$$N_{4\_ring} = 6 + N_{8\_ring} \quad (2)$$

In the case of the hollow polyhedrons, structures cut from the Al_2O_3 crystal were considered to be hollow shell structures with random membered rings. These polyhedrons were defined in terms of their k-gon numbers N_k ($k \leqslant 8$). The initial hollow structures were created on the basis of elimination method that we built different size shape nanocluster (cubic box, sphere, tetrahedron and square pyramid), then eliminated inner core to form hollow shell structure.

3. Results and discussion

3.1. Geometries of hollow $(Al_2O_3)_n$ (n = 10, 12, 16, 18, 24 and 33 clusters

Three types of energetically competitive structures were obtained for hollow Al_2O_3 clusters with n = 10–33. The lowest-energy structures of the fullerene-like Al_2O_3 cage with high symmetry are presented in Fig. 1. The fullerene-like cluster contains

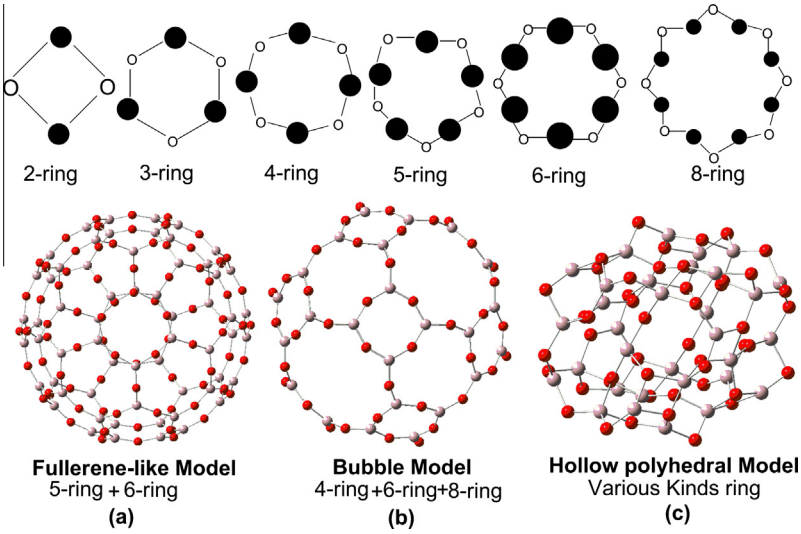

Scheme 1. Three possible model structures.

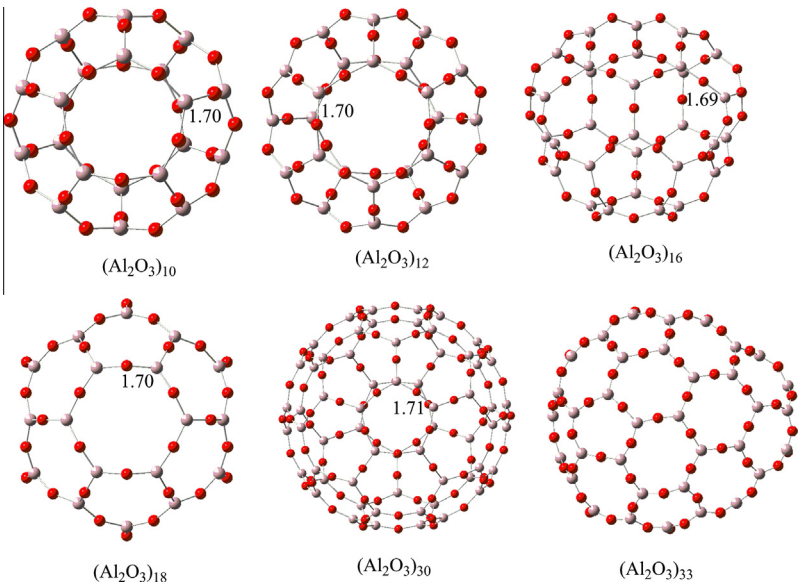

Fig. 1. 3D ball-and-stick representations of the fullerene-like $(Al_2O_3)_n$ hollow clusters optimized at the B3LYP/6-31g* level of theory. The oxygen atoms and aluminum atoms are represented by the small red balls and the large grey balls, respectively. (For interpretation of the references to colour in this figure legend, the reader is referred to the web version of this article.)

threefold aluminum atoms and twofold-coordinated oxygen atom. The average bond lengths of the fullerene-like cage $(Al_2O_3)_n$ decrease with 1.71–1.70 Å as n increases from 11 to 33. Our results are consistent with those obtained in Ref. [12].

The lowest-energy bubble cage structures are shown in Fig. 2. Similar to the case for fullerene-like clusters, these structures also contain threefold-coordinated aluminum atoms and twofold-coordinated oxygen atom. The average bond lengths are about 1.70 Å.

In contrast to the bubble and fullerene—like clusters, the hollow polyhedral cages contain 4-membered Al_2O_2 and other AlO rings with alternating Al and O atoms, as shown in Fig. 3. For $n = 12$, the isomer contains 16 4-membered Al_2O_2 rings, as well as rings with between 6 and 10 membered. It should be noted that the hollow polyhedral clusters contain threefold-, fourfold- and fivefold-coordinated aluminum atoms, as well as twofold- and threefold-coordinated oxygen atom. Therefore, the Al–O bond length can vary from one ring to another. The minimum and the maximum Al–O bond lengths are 1.68 Å and 1.90 Å, respectively; the average bond length is 1.77 Å, which is shorted than that of bulk Al_2O_3 crystal. In bulk α-alumina, three of the Al–O distances are 1.86 Å, whereas the other three are 1.97 Å. In all the $(Al_2O_3)_n$ cage clusters, the Al–O distances are smaller than those in the bulk crystal, which indicates that the Al–O bonding properties in the cage clusters may be a little different from those in the bulk due to the coordination number.

3.2. Relative stability and energies

The relative and binding energies obtained for the chosen lowest-energy structures of different hollow $(Al_2O_3)_n$ (n = 10–33) models are presented in Table 1. From our B3LYP calculations, we found that the polyhedral structural configurations are more stable than the fullerene-like and bubble structural configurations for all hollow clusters sizes studied. The polyhedral structures of hollow

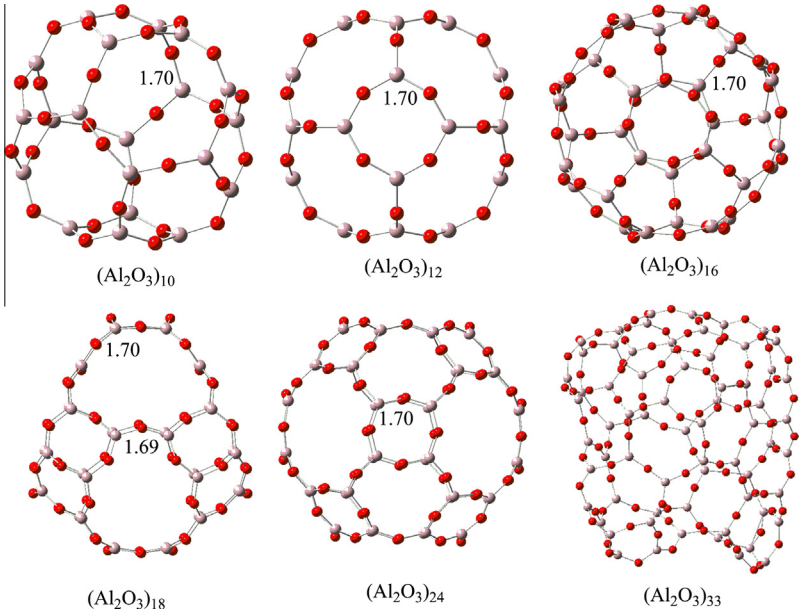

Fig. 2. 3D ball-and-stick representations of the bubble $(Al_2O_3)_n$ hollow clusters optimized at the B3LYP/6-31g* level of theory.

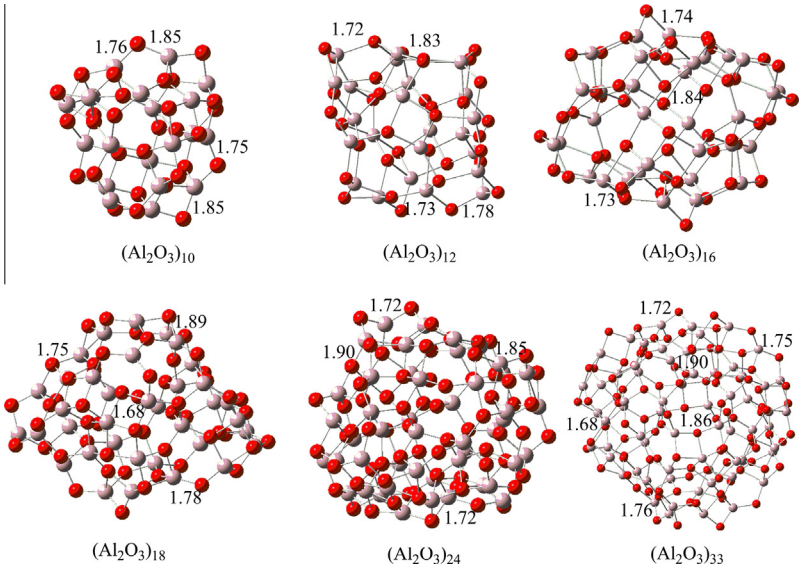

Fig. 3. 3D ball-and-stick representations of the polyhedral $(Al_2O_3)_n$ hollow clusters optimized at the B3LYP/6-31g* level of theory.

$(Al_2O_3)_n$ cluster with $n = 10$ are lower in total energy than the fullerene-like and bubble structures by 0.136 au and 0.146 au, respectively. When $n = 33$, the total energy of polyhedral structure is lower by 1.30 and 1.33 au, respectively. To further investigate the stability of the hollow $(Al_2O_3)_n$ clusters, we calculated the binding energy per Al_2O_3 unit for the equilibrium configuration, which is defined as $E_b = [2nE(Al) + 3nE(O) - E(Al_{2n}O_{3n})]/n$, where E_b is the total binding energy divided by n. Therefore, E_b is the average binding energy per Al_2O_3 unit. From Table 1, the E_b values increase monotonically as the cluster size increases for three type configurations, implying that all three become more stable during the growth process. The binding energies of the polyhedral structure are the largest of three structures. The relative and binding energies of all hollow $Al_{2n}O_{3n}$ clusters are calculated with PBE XC-functionals. The energy ordering does not change when different XC-functions are used. Rahane et al. [9] studied $Al_{2n}O_{3n}$ cluster for

Table 1
Predicted the relative energy (E, au) and binding energies (E_b, eV) per Al_2O_3 unit and HOMO–LUMO Gap (E_g, eV) of optimal cage structure for Al_2O_3 hollow clusters obtained by DFT calculations with B3LYP, PBE density functionals.

Alumina clusters	Cage type	Sym.	B3LYP			PBE	
			E	E_b	E_g	E_b	E_g
$(Al_2O_3)_n$ $n = 10$ 10a	Fullerene-like	I_h	−7108.8872	34.82	5.19	28.65	3.49
$(Al_2O_3)_n$ $n = 10$ 10b	Bubble	D_{2d}	−7108.8769	34.79	5.18	28.60	3.49
$(Al_2O_3)_n$ $n = 10$ 10c	Polyhedral	C_1	−7109.0230	35.19	4.36	29.05	2.77
$(Al_2O_3)_n$ $n = 12$ 12a	Fullerene-like	D_{6d}	−8530.6863	34.87	5.28	28.71	3.58
$(Al_2O_3)_n$ $n = 12$ 12b	Bubble	O_h	−8530.6786	34.85	5.16	28.70	3.52
$(Al_2O_3)_n$ $n = 12$ 12c	Polyhedral	C_1	−8530.9445	35.45	3.36	29.30	2.00
$(Al_2O_3)_n$ $n = 16$ 16a	Fullerene-like	D_{3h}	−11374.2860	34.93	5.32	28.70	3.63
$(Al_2O_3)_n$ $n = 16$ 16b	Bubble	D_{4d}	−11374.2784	34.92	5.32	28.67	3.65
$(Al_2O_3)_n$ $n = 16$ 16c	Polyhedral	C_i	−11374.7752	35.76	5.44	29.58	3.71
$(Al_2O_3)_n$ $n = 18$ 18a	Fullerene-like	D_{6h}	−12796.0778	34.94	5.35	28.78	3.68
$(Al_2O_3)_n$ $n = 18$ 18b	Bubble	C_{2v}	−12796.0446	34.89	5.41	28.77	3.78
$(Al_2O_3)_n$ $n = 18$ 18c	Polyhedral	D_{2d}	−12796.7135	35.90	4.21	29.71	2.66
$(Al_2O_3)_n$ $n = 24$ 24a	Fullerene-like	D_{6d}	−17061.4670	34.98	5.32	28.89	3.71
$(Al_2O_3)_n$ $n = 24$ 24b	Bubble	O_h	−17061.4485	34.95	5.47	28.83	3.83
$(Al_2O_3)_n$ $n = 24$ 24c	Polyhedral	C_1	−17062.3143	35.94	3.88	29.43	1.75
$(Al_2O_3)_n$ $n = 33$ 33a	Fullerene-like	C_i	−23459.5533	35.01	5.31	28.92	3.42
$(Al_2O_3)_n$ $n = 33$ 33b	Bubble	C_1	−23459.5249	34.98	4.99	28.86	3.74
$(Al_2O_3)_n$ $n = 33$ 33c	Polyhedral	C_1	−23460.8597	36.08	3.05	29.92	1.48

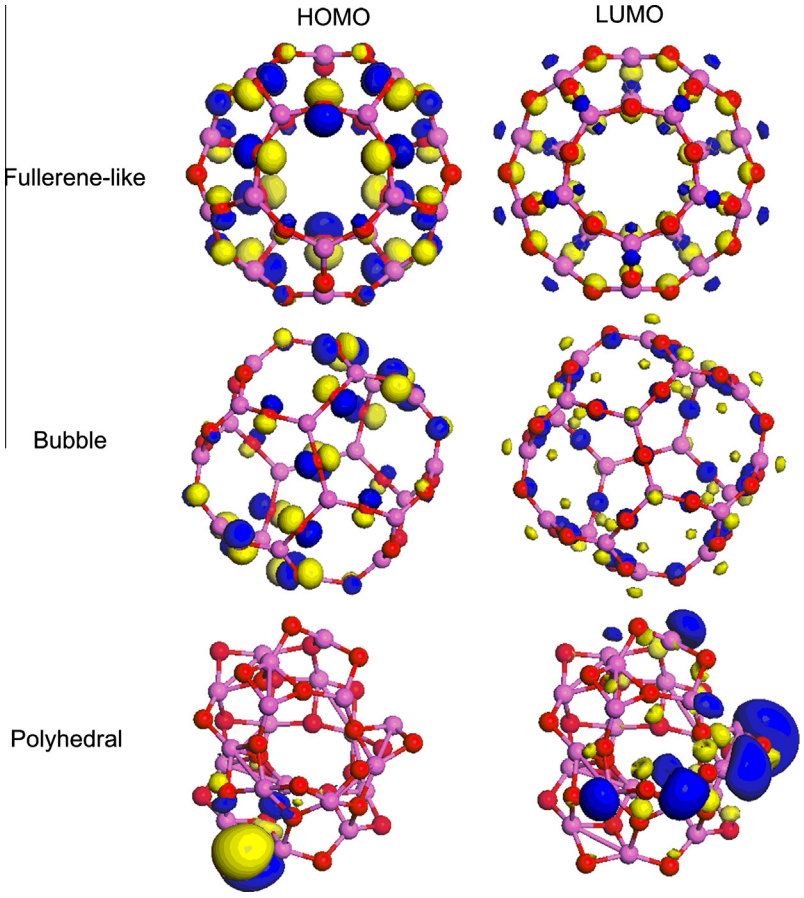

Fig. 4. HOMO and LUMO of three hollow $(Al_2O_3)_{10}$ cluster structures.

n = 1–10 at the PBE level. The BE for the relaxed bulk fragment of Al_2O_3 is 29.8 eV for n = 10, which is significantly higher than the value of 0.7 eV for out lowest energy isomer of n = 10. For comparison, the calculated bulk value of the cohesive energy and the experimental value in α-alumina are 32.3 eV and 31.8 eV, respectively. The tendencies are obtained as expected, since polyhedral hollow structure has more surface atoms and less coordination number.

3.3. Electronic structure and properties

Although polyhedral structures have high thermodynamic stability, the kinetic factors should also be considered. The difference in energy between the highest occupied (HOMO) and the lowest unoccupied (LUMO) molecular orbitals was given in Table 1. All the fullerene-like and bubble structure hollow Al_2O_3 clusters have large HOMO–LUMO gap energies (5.31 eV for fullerene-like $(Al_2O_3)_{33}$ and 4.99 eV for bubble $(Al_2O_3)_{33}$), giving them high kinetic stability. However, the calculated HOMO–LUMO gaps vary between 4.36 eV and 3.05 eV for polyhedral hollow cluster, which are lower than for the other structures. To understand the electron behavior in these configurations, we plotted the HOMO and LUMO of hollow $(Al_2O_3)_{10}$ cluster in Fig. 4. It is evident that the regions of electron density of the HOMO for the fullerene-like and bubble clusters are located on the cage surface, mainly dominated by the oxygen 2p atomic orbitals, whereas the LUMO is mostly contributed by the oxygen 3s atomic orbitals and the aluminum 2p atomic orbitals. The HOMO of the polyhedral cluster is mainly distributed from O_{2p} state on the surface as well as the inferior sites. The LUMO arise from the oxygen 3s atomic orbitals and the aluminum 2p atomic orbitals. Next, we analyzed the charges of hollow $Al_{2n}O_{3n}$ clusters by Mulliken analysis. For all cluster sizes studied, charge transfer occurs from the Al atom to the O atom in hollow $Al_{2n}O_{3n}$ clusters. For fullerene-like and bubble clusters, the Al atom loses the average charge of 1.02e and the O atom gains the average charge of 0.68e. Similar situation is observed in polyhedral structures. For polyhedral $(Al_2O_3)_{33}$, the Al atoms lose the charge of 1.14e and the o atoms get the charge of 0.76e. This suggests that the Al site of polyhedral structures has a stronger Lewis acidity than that of fullerene-like and bubble structures.

3.4. IR and Raman spectra

The infrared (IR) absorption spectra of the hollow $(Al_2O_3)_n$ clusters were computed at the B3LYP/6-31g* level (Fig. 5). Several relatively strong peaks in fullerene-like $(Al_2O_3)_n$ cluster are 1099 (the strongest), 443 and 269 cm^{-1}, corresponding to the existence of Al–O stretch mode. Similar to that of fullerene-like, the calculations predicted five IR-active vibrational frequencies of bubble $(Al_2O_3)_n$ cluster at 324, 386, 428, 579 (relatively weak intensity) and 1099 cm^{-1} (the strongest). For hollow polyhedral $(Al_2O_3)_n$ cluster, each of their spectra can be roughly partitioned into two bands (from 600 to 800 cm^{-1}, and from 800 to 1000 cm^{-1}). The two bands are contributed by the vibrations of the Al–O stretch mode with large absorption intensities. Among them, the strongest absorption peaks locate at 880 cm^{-1} as compared to the bulk IR mode at 822 cm^{-1} for α-alumina and 738.6 cm^{-1} for γ-alumina. As we all know, the highest vibrational frequency is larger in cluster than in the bulk because the mean Al–O bond length in clusters is shorter than in bulk. However, this results of the highest intensity IR frequency for polyhedral hollow $(Al_2O_3)_n$ do not agree well with the available experimental results [20] that the highest intensity absorption peaks locate at 700 cm^{-1}. It is attributed by the synthesized thickness of Al_2O_3 as well as some nanopores on the Al_2O_3 hollow spheres. These will be studied further in the future.

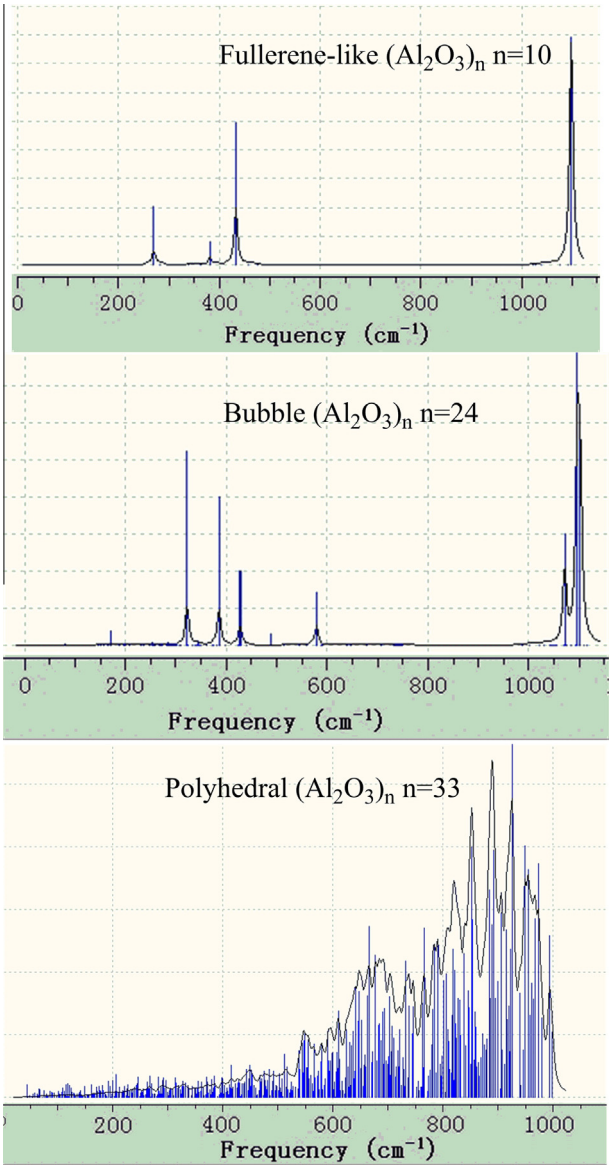

Fig. 5. Calculated IR vibrational spectra.

4. Conclusion

Using DFT, the structures, stabilities and binding energies of three hollow $(Al_2O_3)_n$ (n = 10, 12, 16, 18, 24 and 33) clusters were studied. The calculations of total energy and binding energy revealed that the polyhedral structures are more stable than the fullerene-like and bubble clusters. In polyhedral structures clusters, the binding energy increases as the cluster size increases. For a given size, the HOMO–LUMO gaps of fullerene-like and bubble clusters are larger than that of the polyhedral cluster. On the basis of these results, polyhedral clusters are good models for predicting or interpreting the novel properties of hollow Al_2O_3 nanoshell. We anticipate that the present DFT study will facilitate the experimental synthesis for the nano shells.

Acknowledgements

This work is supported by the National Science Foundation of China, Grant Number: (No. 20873107) and the National Fund for Fostering Talents of Basic Science (NFFTBS; No. J1030415).

References

[1] E. Bernardo, P. Colombo, E. Pippel, J. Woltersdorf, Novel mullite synthesis based on alumina nanoparticles and a preceramic polymer, J. Am. Ceram. Soc. 89 (2006) 1577–1583.

[2] J. Emsley, The Elements, Oxford University Press, Oxford, 1998.

[3] P.M. Arnal, M. Comotti, F. Schüth, High-temperature-stable catalysts by hollow sphere encapsulation, Angew. Chem. Int. Ed. 45 (2006) 8224–8227.

[4] Y.W. Wang, W.J. Tseng, A novel technique for synthesizing nanoshell hollow alumina particles, J. Am. Ceram. Soc. 92 (2009) S32–S37.

[5] J.F. Li, Y.F. Huang, Y. Ding, Z.L. Yang, S.B. Li, X.S. Zhou, F.R. Fan, W. Zhang, Z.Y. Zhou, D.Y. Wu, B. Ren, Z.L. Wang, Z.Q. Tian, Shell-isolated nanoparticle-enhanced Raman spectroscopy, Nature 464 (2010) 392–395.

[6] A. Martinez, L.E. Sansores, R. Salcedo, F.J. Tenorio, J.V. Ortiz, Al_3O_n and $Al_3O_n^-$ ($n = 1–3$) clusters: structures, photoelectron spectra, harmonic vibrational frequencies, and atomic charges, J. Phys. Chem. A 106 (2002) 10630–10635.

[7] M.-M. Zhong, X.-Y. Kuanga, H.-Q. Wanga, H.-F. Li, Y.-R. Zhao, Density functional study of the structural and electronic properties of tetra-aluminum oxide $Al_4O_n^{\lambda}$ ($3 < n < 8$, $\lambda = 0, -1$) clusters, Mol. Phys. 109 (2011) 603–612.

[8] S.M. Woodley, Atomistic and electronic structure of $(X_2O_3)_n$ nanoclusters, $n = 1–5$, X = B, Al, In, Ga and Tl, Proc. R. Soc. A 467 (2011) 2020–2042.

[9] A.B. Rahane, M.D. Deshpande, V. Kumar, Structural and electronic properties of $(Al_2O_3)_n$ clusters with $n = 1–10$ from first principles calculations, J. Phys. Chem. C 115 (2011) 18111–18121.

[10] R. Li, L.J. Cheng, Structural determination of $(Al_2O_3)_n$ ($n = 1–7$) clusters based on density functional calculation, Comp. Theor. Chem. 996 (2012) 125–131.

[11] V.V. Karasev, A.A. Onischuk, O.G. Glotov, A.M. Baklanov, A.G. Maryasov, V.E. Zarko, V.N. Panfilov, A.I. Levykin, K.K. Sabelfeld, Formation of charged aggregates of Al_2O_3 nanoparticles by combustion of aluminum droplets in air, Combust. Flame 138 (2004) 40–54.

[12] J. Sun, W.C. Lu, W. Zhang, L.Z. Zhao, Z.S. Li, C.C. Sun, Theoretical study on $(Al_2O_3)_n$ ($n = 1–10$ and 30) fullerenes and H_2 adsorption properties, Inorg. Chem. 47 (2008) 2274–2279.

[13] S. Hamad, C.R.A. Catlow, Structure and properties of ZnS nanoclusters, J. Phys. Chem. B 109 (2005) 2703–2709.

[14] C.R.A. Catlow, S.T. Bromley, S. Hamad, M. Mora-Fonz, A.A. Sokol, S.M. Woodley, Modelling nano-clusters and nucleation, Phys. Chem. Chem. Phys. 12 (2010) 786–811.

[15] B. Delley, An all-electron numerical method for solving the local density functional for polyatomic molecules, J. Chem. Phys. 92 (1990) 508–517.

[16] B. Delley, From molecules to solids with the DMol3 approach, J. Chem. Phys. 113 (2000) 7756–7764.

[17] A.D. Becke, A multicenter numerical integration scheme for polyatomic molecules, J. Chem. Phys. 88 (1988) 2547–2553.

[18] C. Lee, W. Yang, R.G. Parr, Development of the Colle-Salvetti correlation-energy formula into a functional of the electron density, Phys. Rev. B 37 (1988) 785–789.

[19] E. Spano, S. Hamad, C.R.A. Catlow, Computational evidence of bubble ZnS clusters, J. Phys. Chem. B 107 (2003) 10337–10340.

[20] R.J. Liu, Y.J. Li, H. Zhao, F.Y. Zhao, Y.Q. Hu, Synthesis and characterization of Al_2O_3 hollow spheres, Mater. Lett. 62 (2008) 2593–2595.